BOUT++2023 Workshop

Development and application of LPD model based on BOUT++

Yue Wang[1], Chaofeng Sang[1,†], Nami Li[2], Yao Huang[3], Mingzhou Zhang[1]

[1]School of Physics, Dalian University of Technology, Dalian 116024, China
[2] Lawrence Livermore National Laboratory, Livermore, CA 94550, USA
[3]Institute of Plasma Physics Chinese Academy of Sciences, Hefei 230031, China

Email: sang@dlut.edu.cn or dutwangy@mail.dlut.edu.cn

Outline

1. Background & Research Significance
2. Mesh & Physical Model
3. Numerical Results
4. Conclusions and Future Plans

Outline

1. **Background & Research Significance**
2. Mesh & Physical Model
3. Numerical Results
4. Conclusions and Future Plans

The introduction of LPD(linear plasma device)

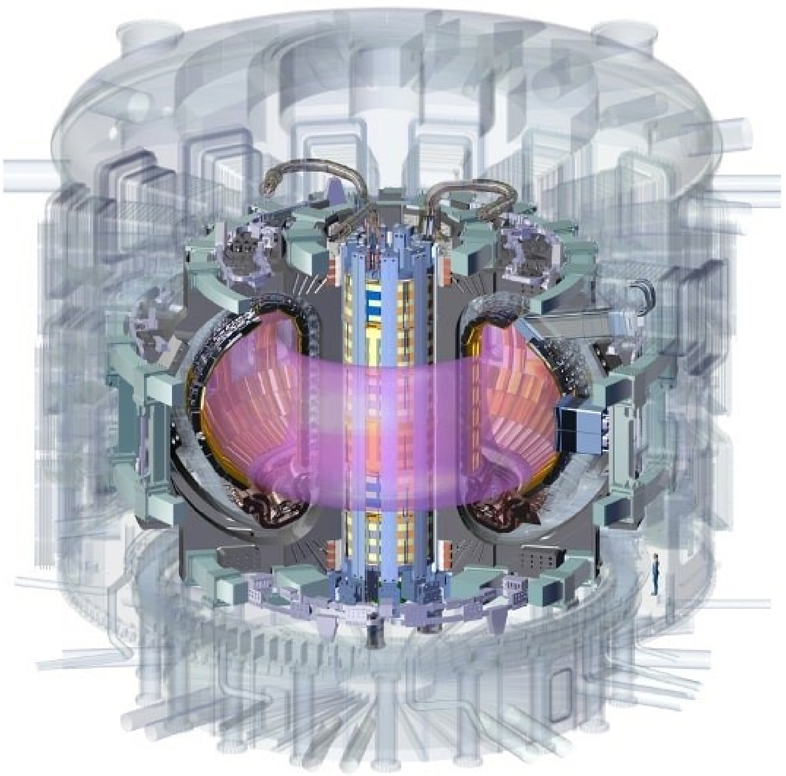

- Long experiment period
- high cost and time-consuming
- Parameters and rules are complex

LPD, which is also called linear divertor plasma simulator

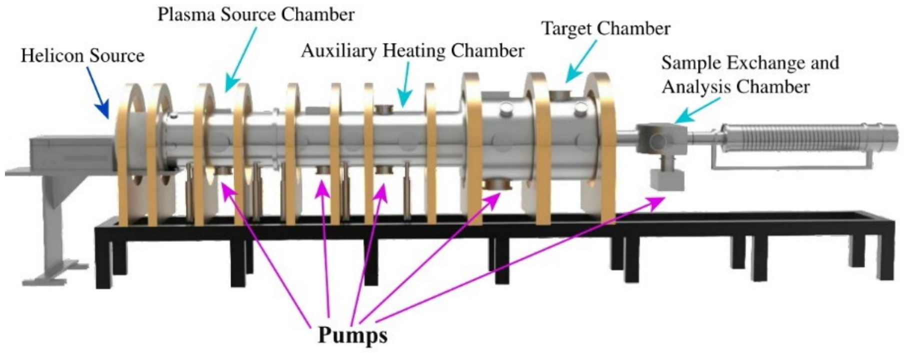

- Easy to upgrade
- Short experimental period and low cost
- Single parameter, suitable for principle experiments
- simplified environment

The LPDs have been applied to investigate the high particle/heat flux irradiation [1], erosion of the materials [2] , fuel retention [3] and PMI[4].

[1] G. De et al , *Fusion Eng. Des*, **88** (2013) 483
[2] J. van Rooij et al, J. Nucl. Mater, **415** (2011) S137
[3] G.H. Lu et al, Fusion Sci. Technol, **71** (2017) 177
[4] J. Rapp et al, Fusion Eng. Des. **85** (2010) 1455

Basic information of MPS-LD linear plasma device

The device is about 3m long and consists of 11 coils

parameters	Desired Value
Magnetic field (axis)	3000 G
Ion temperature	1-20 eV
Electron temperature	1-20 eV
Electron density	10^{18}-$10^{19}/m^3$
Ion flux	10^{21}-$10^{23}/m^2$s
Ion fluence	up to 10^{26} m^{-2} per exposure
Target bias voltage	< 300 V
Target (sample) temperature	300-1000K
Diameter of plasma column	< 10 cm
Operational pressure	down to 10^{-2}Pa
Vacuum pressure	10^{-4}Pa

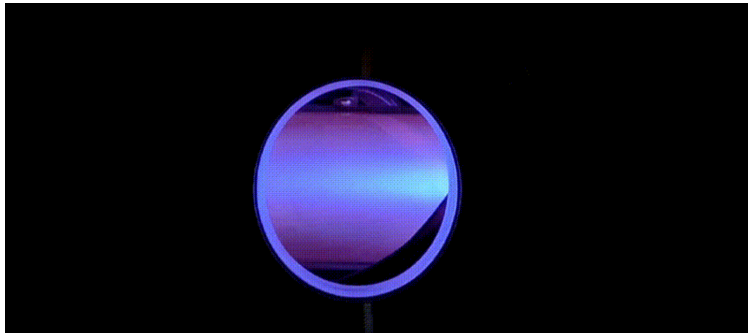

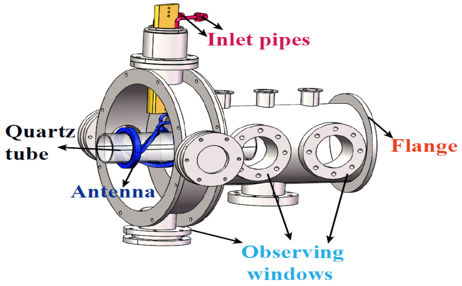

Result of plasma source discharge

- PMIs, e.g. irradiation damage, fuel retention
- Edge plasma transport
- High density plasma source
- Plasma heating

Simulation of Plasma Transport in Linear Device

- The plasma will be transported along magnetic lines in the magnetic field, undergo complex atomic and molecular processes, and eventually reach the divertor target;
- The plasma is similar to the plasma behavior of the scraping layer in tokamak, and the scraping layer and divertor are simulated in the laboratory.
- In order to understand the plasma transport in MPS-LD device and accurately predict the energy flow and particle flow deposited on the divertor target, it is urgent to carry out relevant numerical simulation research.

Code	Device
SOLPS	MPEX，MPS-LDMagnum-PSI, MAGPIE, Proto-MPEX, GyM
EMC3-Eirene	MPEX
B2.5-Eunomia	Pilot-PSI, Magnum-PSI
SolEdge2D-Eirene	Pilot-PSI
BOUT++ Hermes	Magnum-PSI
LINDA	NAGDIS-II

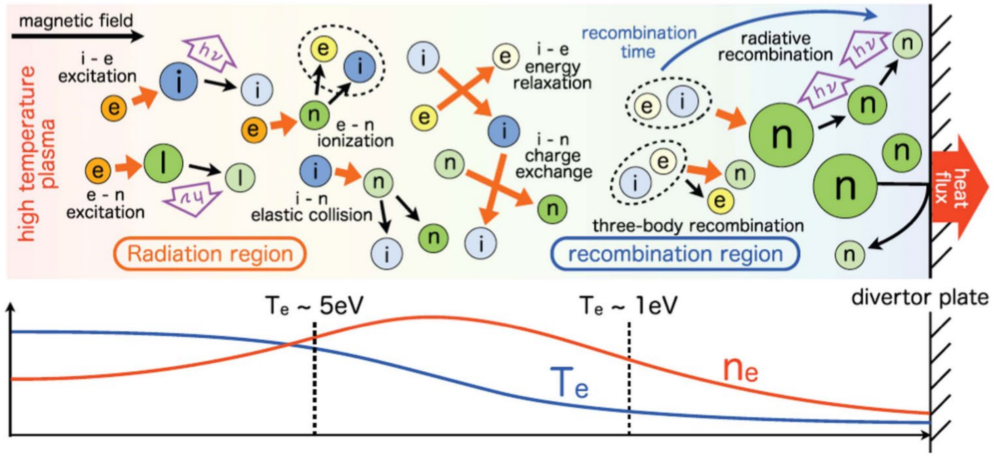

BOUT + + for Tokamak Simulation

EAST

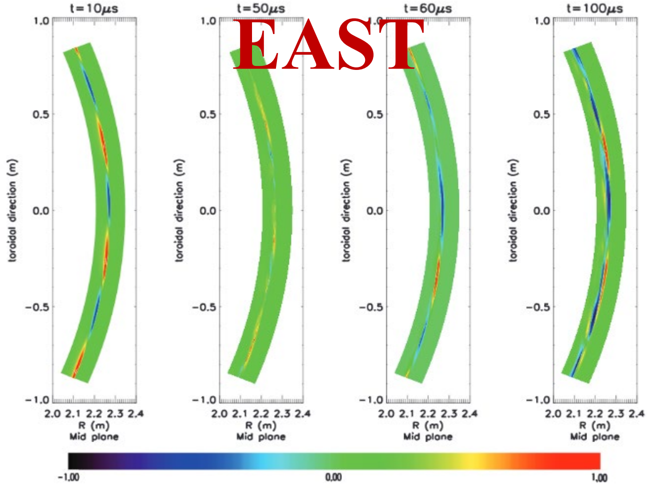

Nucl. Fusion 55 (2015) 113030

C-Mod

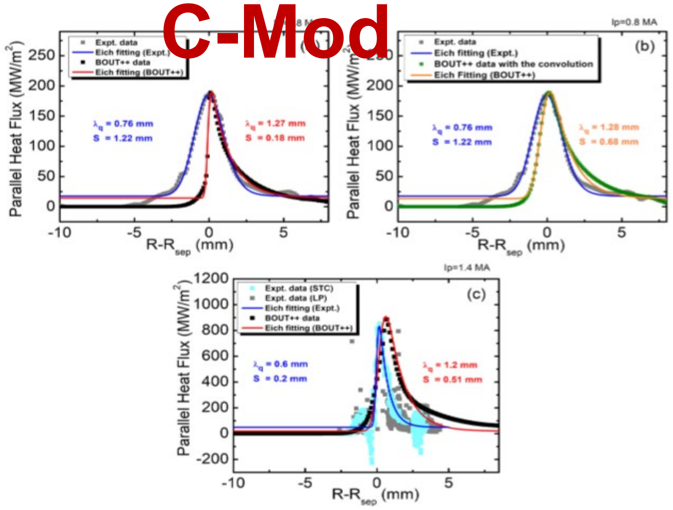

AIP Adv., 10 (2020) 015222

KSTAR

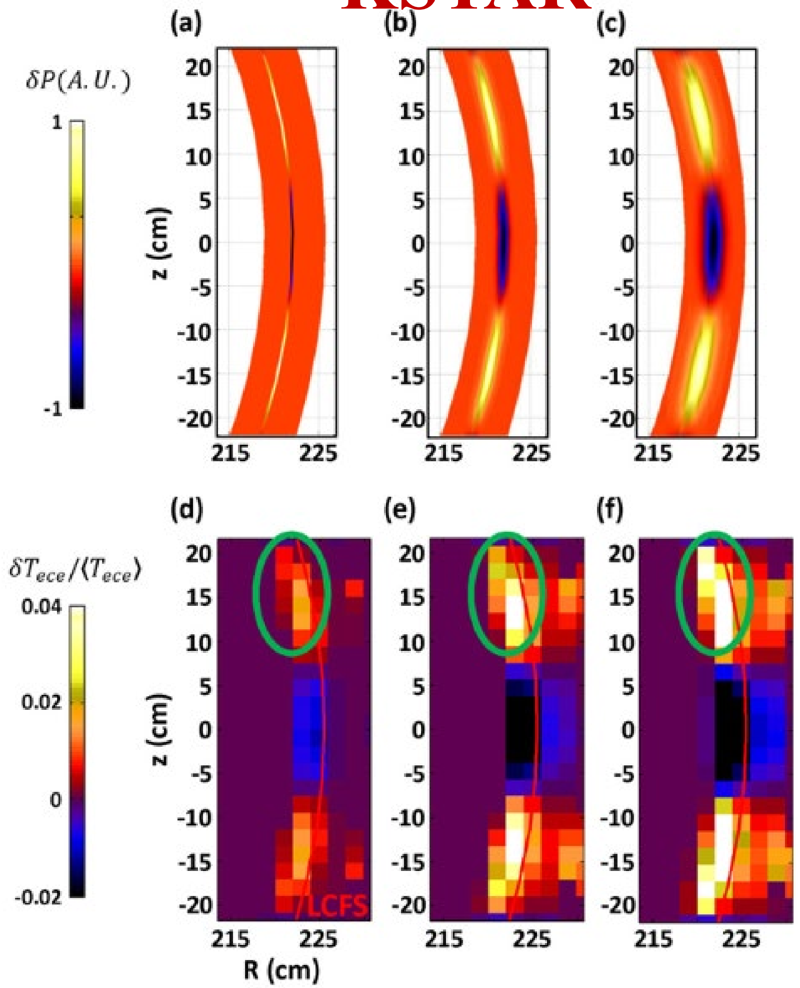

DIII-D

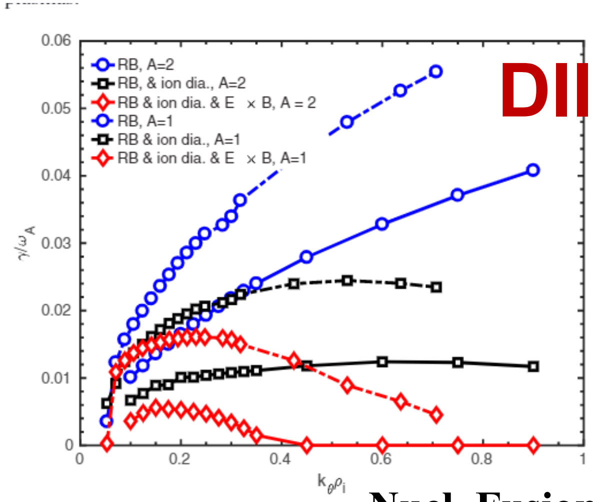

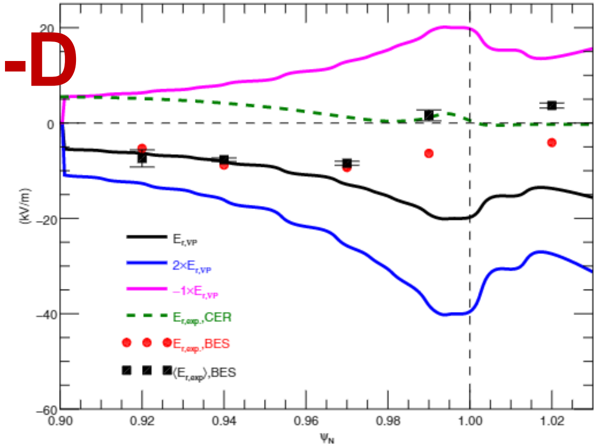

Nucl. Fusion 58 (2018) 026026

Nucl. Fusion 54 (2014) 09300

Necessity of Simulating Linear Device Based on BOUT++

BOUT++

- efficient parallel code, which allows obtaining the numerical solution faster
- Separation of source code from user application code
- **Modularization of physical algorithms**
- **Support open source**

Linear device

- A steady-state plasma beam can be formed by constructing a steady-state magnetic field to construct a **divertor-like plasma environment**
- low cost, short cycle, easy diagnosis and single and controllable experimental variables
- Existing device

LPD module simulating Linear device based on BOUT++

- ✓ Plasma parameters near the target can be obtained
- ✓ **We know the dependence of plasma parameters near the target on the plasma source,**
- ✓ **A New Numerical Tool for Linear Device Modeling**

Outline

LPD module simulates MPS-LD device

LPD model

LD-MCC magnetic field calculation code

- Calculate the magnetic field configuration
- Magnetic field information is stored as standard magnetic field data file

Mesh generator code

- Standard data storage interface program
- Generate mesh files readable by BOUT++

2D Transport model

- Reduce Braginskii equation

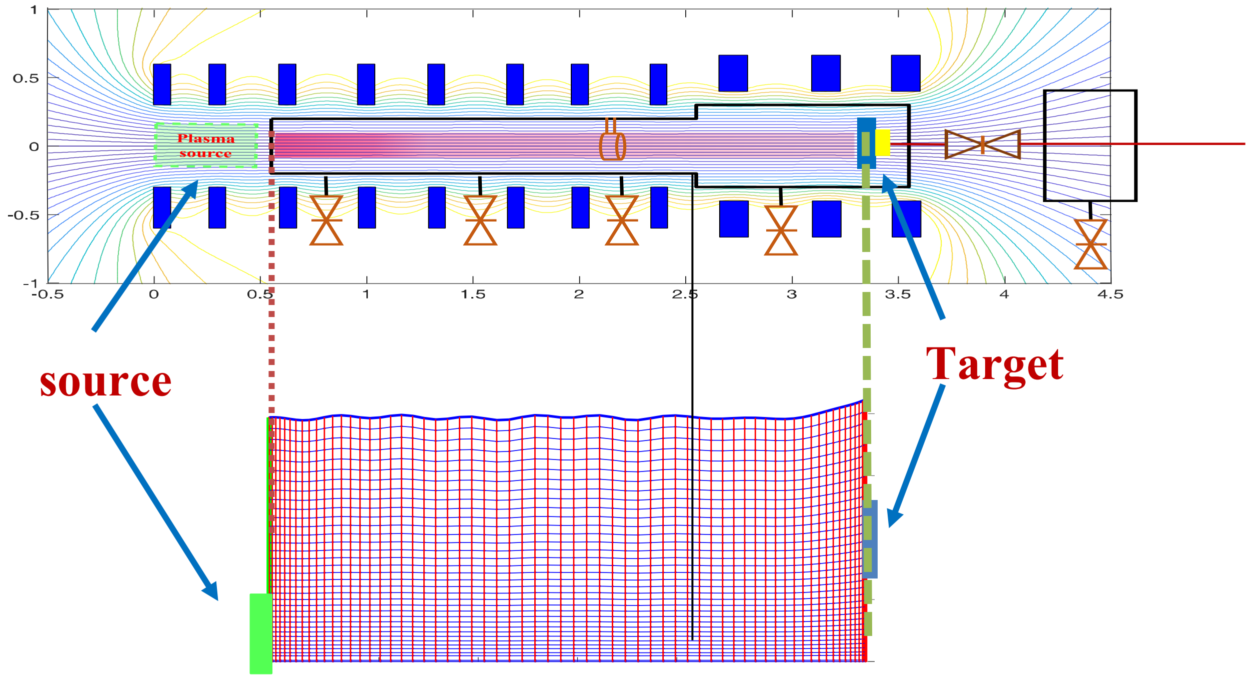

Non-uniform grids are used

The simulation of the plasma transport in MPS-LD device is modeled by the LPD module of BOUT++

LD-MCC magnetic field calculation code

The magnetic vector potential $\vec{A}(r, \varphi, z)$ in the cylindrical coordinate system can be calculated by circular current loop:

$$\vec{A}(\mathrm{r},\varphi,\theta) = \frac{\mu I_0 a}{\pi K_c [r_c a \sin\theta]^{\frac{1}{2}}} \left[\left(1 - \frac{K_c}{2}\right) K(K_c) - E(K_c) \right] \hat{\varphi}$$

$$k_c{}^2 = \frac{4 r_c a \sin\theta}{r_c{}^2 + a^2 + 2 r_c a \sin\theta}$$

where $K(k_c)$, $E(k_c)$ are complete elliptic integral functions of the first and second types

The components of the magnetic field are expressed as:

$$B_R = -\frac{1}{R}\frac{\partial\psi}{\partial z}, \quad B_z = -\frac{1}{R}\frac{\partial\psi}{\partial R}$$

The total magnetic field *B* in the LPD is

$$B_n = \sqrt{B_{n,r}{}^2 + B_{n,z}{}^2} \qquad B = \sum_{n=1}^{11} B_n$$

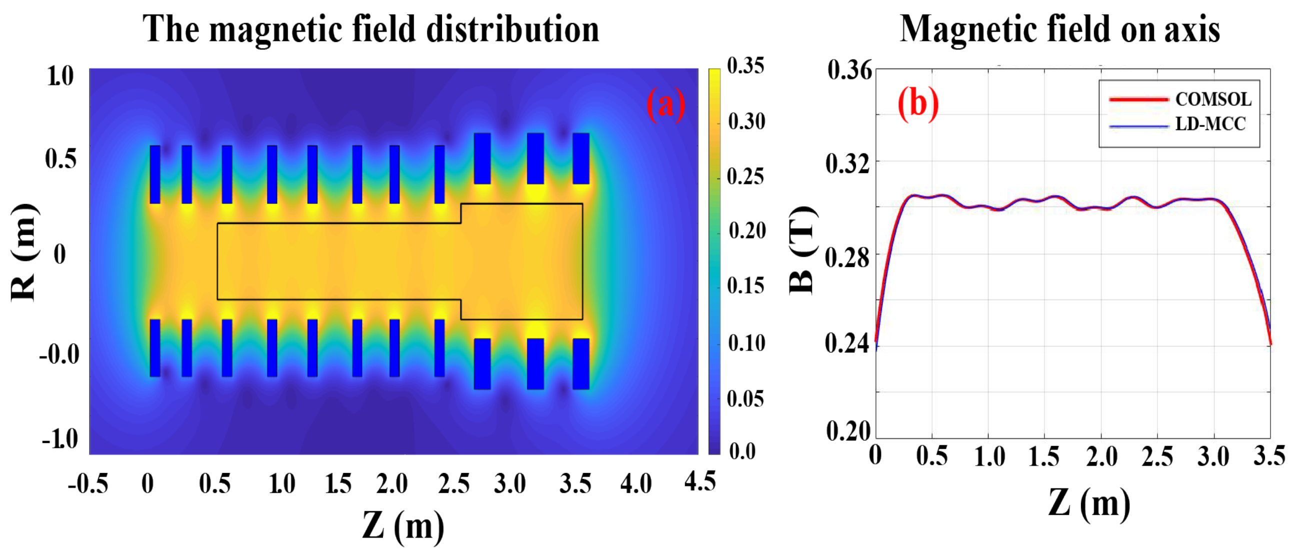

By using the location and current of each coil in MPS-LD, see table 2 in [1], LPD-MCC (Linear Plasma Devices-Magnetic field Configuration Calculation) can be verified by benchmarking against the COMSOL calculation.

[1] C. Sun et al, Fusion Engineering and Design 162 (2021) 112074

2D Transport model

Continuity equations

$$\frac{\partial N_i}{\partial t} + \nabla_\parallel (V_{\parallel i} N_i) - \nabla_\perp \cdot (D_\perp \nabla_\perp N_i) = S_I^p - S_{rec}^p$$

$$\frac{\partial N_{He^+}}{\partial t} + \nabla_\parallel (V_{\parallel He^+} N_{He^+}) - D_{\perp He^+} \nabla_\perp^2 N_{He^+} = S_I^{He} - S_{rec}^{He}$$

Momentum equations

$$\frac{\partial V_{\parallel i}}{\partial t} + V_{\parallel i} \nabla_\parallel V_{\parallel i} - \frac{4}{3 N_i M_i} \nabla_\parallel (\eta_i \nabla_\parallel V_{\parallel i}) = -\frac{\nabla_\parallel P}{N_i M_i} + \frac{D_\perp}{N_i} \nabla_\perp N_i \cdot \nabla V_{\parallel i} - \frac{N_i + N_{He^+}}{N_i} \nu_I V_{\parallel i} - F_i$$

$$\frac{\partial V_{\parallel He^+}}{\partial t} + V_{\parallel He^+} \nabla_\parallel V_{\parallel He^+} - \frac{4}{3 N_{He^+} M_{He^+}} \nabla_\parallel (\eta_{He^+}^0 \nabla_\parallel V_{\parallel He^+}) = -\frac{\nabla_\parallel P_{He^+}}{N_{He^+} M_{He^+}} + \frac{D_{\perp He^+}^c}{N_{He^+}} \nabla_\perp N_{He^+} \cdot \nabla V_{\parallel He^+} - \frac{N_i + N_{He^+}}{N_{He^+}} \nu_{He^+} V_{\parallel He^+} + \frac{N_i M_i}{N_{He^+} M_{He^+}} F_i$$

Energy equations

$$\frac{\partial T_e}{\partial t} - \frac{2}{3 N_e} \nabla_\parallel (\kappa_{\parallel e}^c \nabla_\parallel T_e) = \frac{2}{3} \chi_{\perp e} \nabla_\perp^2 T_e - \nu_I \left(T_e + \frac{2}{3} W_I \right) - \nu_{He^+} \left(T_e + \frac{2}{3} W_{He^+} \right) - \frac{2 m_e}{M_i} \frac{T_e - T_i}{\tau_e} - \frac{2 m_e}{M_{He}} \frac{T_e - T_{He^+}}{\tau_e^{He^+}}$$

$$\frac{\partial T_i}{\partial t} + V_{\parallel i} \nabla_\parallel T_i + \frac{2}{3} T_i \nabla_\parallel V_{\parallel i} - \frac{2}{3 N_i} \nabla_\parallel (\kappa_{\parallel i}^c \nabla_\parallel T_i) = \frac{2}{3} \chi_{\perp i} \nabla_\perp^2 T_i - \frac{N_i + N_{He^+}}{N_i} \nu_I T_i + \frac{N_i + N_{He^+}}{N_i} \frac{2 m_e}{M_i} \frac{T_e - T_i}{\tau_e} + \frac{2 M_i}{M_{He}} \frac{T_{He^+} - T_i}{\tau_{iHe^+}}$$

$$\frac{\partial T_{He^+}}{\partial t} + \nabla_\parallel T_{He^+} + \frac{2}{3} T_{He^+} \nabla_\parallel V_{\parallel He^+} - \frac{2}{3 N_{He^+}} \nabla_\parallel (\chi_{\perp He^+} \nabla_\parallel T_{He^+}) = \frac{2}{3} \chi_{\perp He^+}^c \nabla_\perp^2 T_{He^+} - \frac{N_i + N_{He^+}}{N_{He^+}} \left(\nu_{He^+} T_{He^+} - \frac{2 m_e}{M_{He}} \frac{T_e - T_{He^+}}{\tau_e^{He^+}} \right) + \frac{2 M_i N_i}{N_{He^+} M_{He}} \frac{T_i - T_{He^+}}{\tau_{i,He^+}}$$

Neutral equations

$$\frac{\partial N_a}{\partial t} + \nabla_Z (V_a N_a) = S_{rec}^p - S_I^p \qquad \frac{\partial N_{He}}{\partial t} + \nabla_Z (V_{He} N_{He}) = S_{rec}^{He} - S_I^{He}$$

$$\frac{\partial V_a}{\partial t} = -V_a \nabla_Z V_a - \frac{\nabla_Z P_a}{N_a M_a} \qquad \frac{\partial V_{He}}{\partial t} = -V_{He} \nabla_Z V_{He} - \frac{\nabla_Z P_{He}}{N_{He} M_{He}}$$

axial term
Radial term
Source term
Energy exchange

[1] Li et al , *Comput. Phys. Commun.* **228** (2018) 69
[2] Li et al , *Nucl. Mater. Energy* **12** (2017) 119
[3] Wang et al , *PPCF* **64** (2022) 115010

Boundary conditions applicable to linear devices

Plasma source boundary

- Continuity equations: $N_i|_{Z=0} = N_0 e^{\frac{-(R-a)^2}{2b^2}}$, $\nabla_\parallel N_{He^+}|_{Z=0} = 0$
- Momentum equations: $V_{\parallel i}|_{Z=0} = V_0 e^{\frac{-(R-e)^2}{2f^2}}$, $\nabla_\parallel V_{He^+}|_{Z=0} = 0$
- Energy equations: $\nabla_\parallel T_e|_{Z=0} = \nabla_\parallel T_i|_{Z=0} = T_0 e^{\frac{-(R-c)^2}{2d^2}}$, $\nabla_\parallel T_{He^+}|_{Z=0} = 0$
- Neutral equations: $\nabla_\parallel N_a|_{Z=0} = 0$, $N_{He}|_{Z=0} = N_{He0} e^{\frac{-(R-g)^2}{h^2}}$, $\nabla_\parallel V_{He}|_{Z=0} = V_{He0}$

Gaussian distribution radially

Target boundary

- Continuity equations: $\nabla_\parallel N_i|_{Z=-1} = 0$, $\nabla_\parallel N_{He^+}|_{Z=-1} = 0$
- Momentum equations: $V_{\parallel i}|_{Z=-1} = C_s|_{Z=-1}$, $V_{He^+}|_{Z=-1} = C_s|_{Z=-1}$
- Energy equations: $\nabla_\parallel T_i|_{Z=-1} = \nabla_\parallel T_{He^+}|_{Z=-1} = -q_{sh,i}/(k\kappa_{\parallel i})|_{Z=-1}$

  $\nabla_\parallel T_e|_{Z=-1} = -q_{sh,e}/(k\kappa_{\parallel e})|_{Z=-1}$
- Neutral equations: $\nabla_\parallel N_a|_{Z=-1} = -\frac{\Gamma_a^d}{D_{\parallel a}}$, $\nabla_\parallel N_{He}|_{Z=-1} = -\frac{\Gamma_{He}^d}{D_{\parallel He}}$, $\nabla_\parallel V_{He}|_{Z=-1} = 0$

Sheath boundary conditions

Chamber wall boundary

- Neutral equations: $\nabla_\perp N_a|_{R=-1} = -\frac{\Gamma_a^w}{D_{\perp a}}$, $\nabla_\perp N_{He}|_{R=-1} = -\frac{\Gamma_{He}^w}{D_{\perp He}}$, $\nabla_\parallel V_{He}|_{R=-1} = 0$

Axis boundary

Neumann boundary conditions are used for density, velocity and temperature equations

Outline

A two-point model is applied to analyze the results

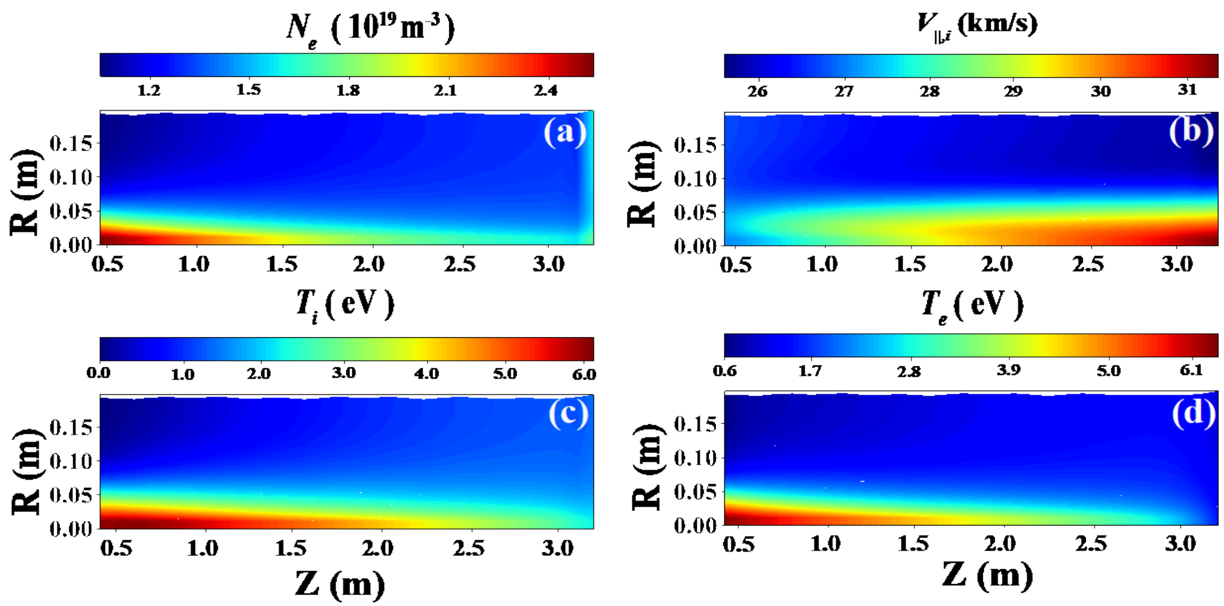

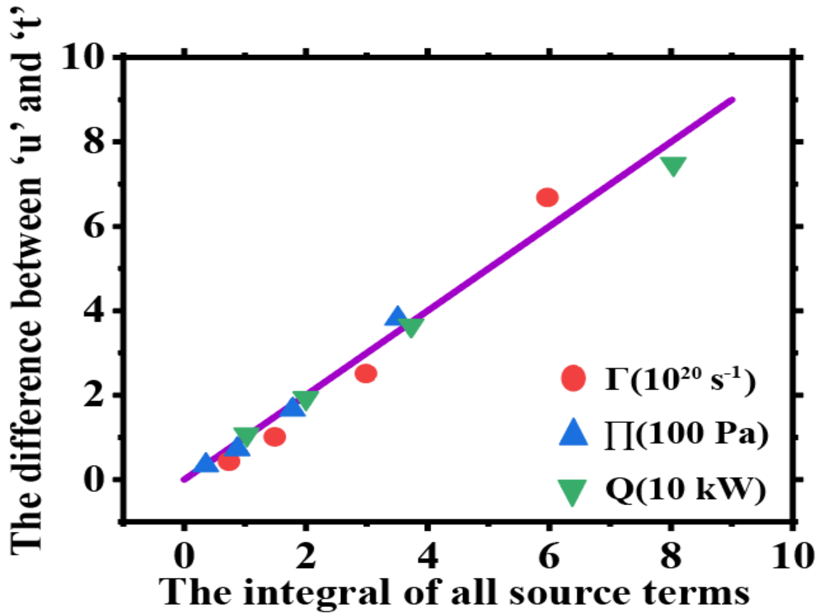

The simulated main plasma parameters are shown

The differences of particle, momentum and energy fluxes between the upstream and target **are almost identical to the integration of each term**

Continuity equations: $\Gamma_t - \Gamma_u = \int_u^t S_\Gamma^R dz + \int_u^t S_\Gamma^N dz$

Momentum equations: $\Pi_t - \Pi_u = \int_u^t M_i S_\Pi^R dz + \int_u^t M_i S_\Pi^N dz$

Energy equations: $Q_{t,\alpha} - Q_{u,\alpha} = \int_u^t S_{Q,\alpha}^R dz + \int_u^t S_{Q,\alpha}^N dz \pm \int_u^t q_\alpha dz$

Wang Yue et al , Plasma Phys. Control. Fusion 64 (2022) 115010

Simulation Results verification

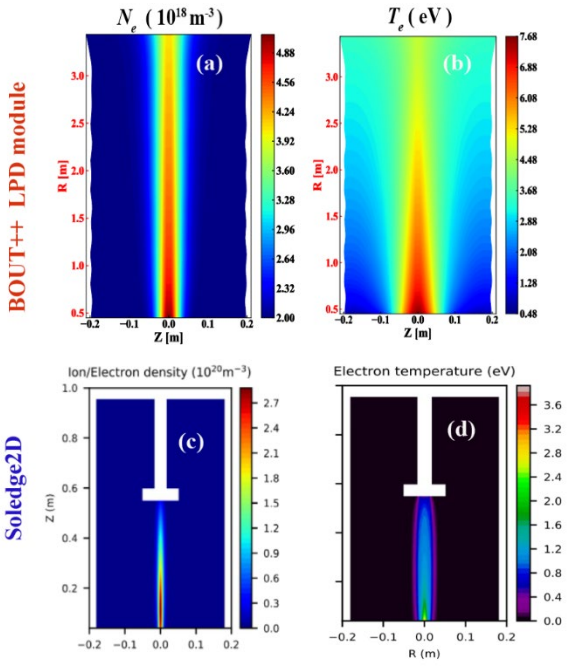

PPCF 60 (2018) 125009

The results of BOUT + + were **qualitatively compared** with those of a simulated Pilot-PSI device using SOLE2D-Eirene

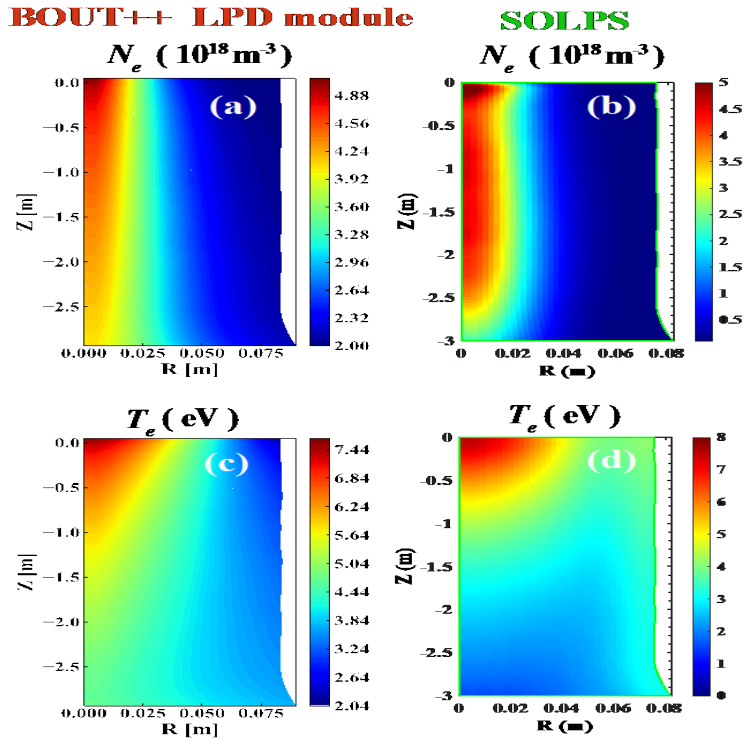

In the radial direction, *Ne* gradually decreases toward the wall, and the distribution is similar to that of the **Magnum-PSI experiment**

PPCF 63 (2021) 095006

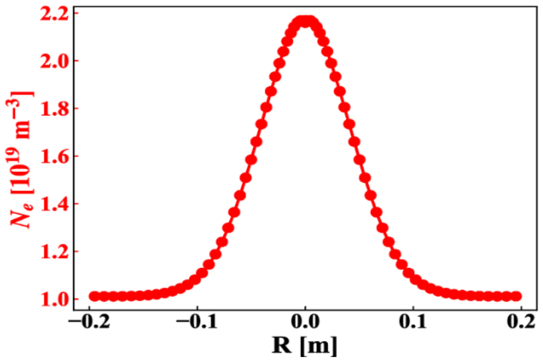

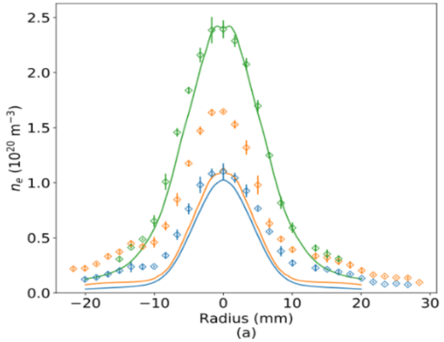

quantitative comparison between BOUT++ and SOLPS-ITER modeling are shown

The consistency of the trend of the main parameters

Y. J Zhang, Nuclear Materials and Energy 33 (2022) 101280

Effect of Transport Coefficient on Thermal Load of Target

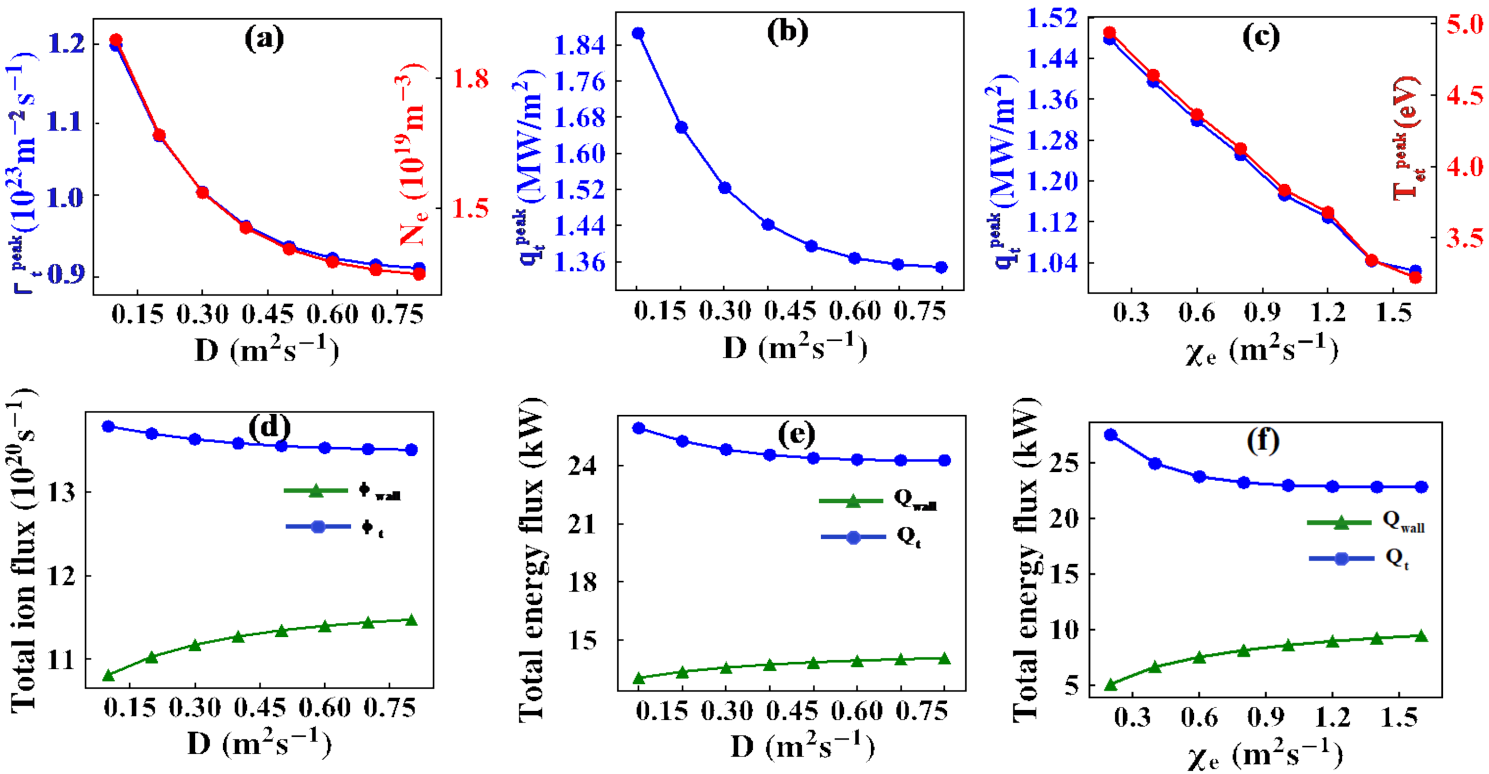

The variation of the main plasma parameters at the target with $D_\perp$ and $\chi_{\perp i,e}$

The increase of $D_\perp$ will lead to a significant decrease in N_e at the target, resulting in a decrease Γ_t^{peak}, but has little effect on T_{et}^{peak}, so Q_{wall} is enhanced, resulting in a decrease in q_t^{peak} and a corresponding decrease in Q_t.

$\chi_{\perp i,e}$ only affects q. Q_{wall} increases with the increase of $\chi_{\perp i,e}$, while Q_t decreases with the increase of $\chi_{\perp i,e}$.

- Smaller $D_\perp$ and $\chi_{\perp i,e}$ are beneficial to suppress the radial transport, reduce the beam spot width, and increase the particle flux and heat flux reaching the target. This requires enhance magnetic field strength to obtain stronger particle flux and plasma energy flux density.

Evolution of helium ions

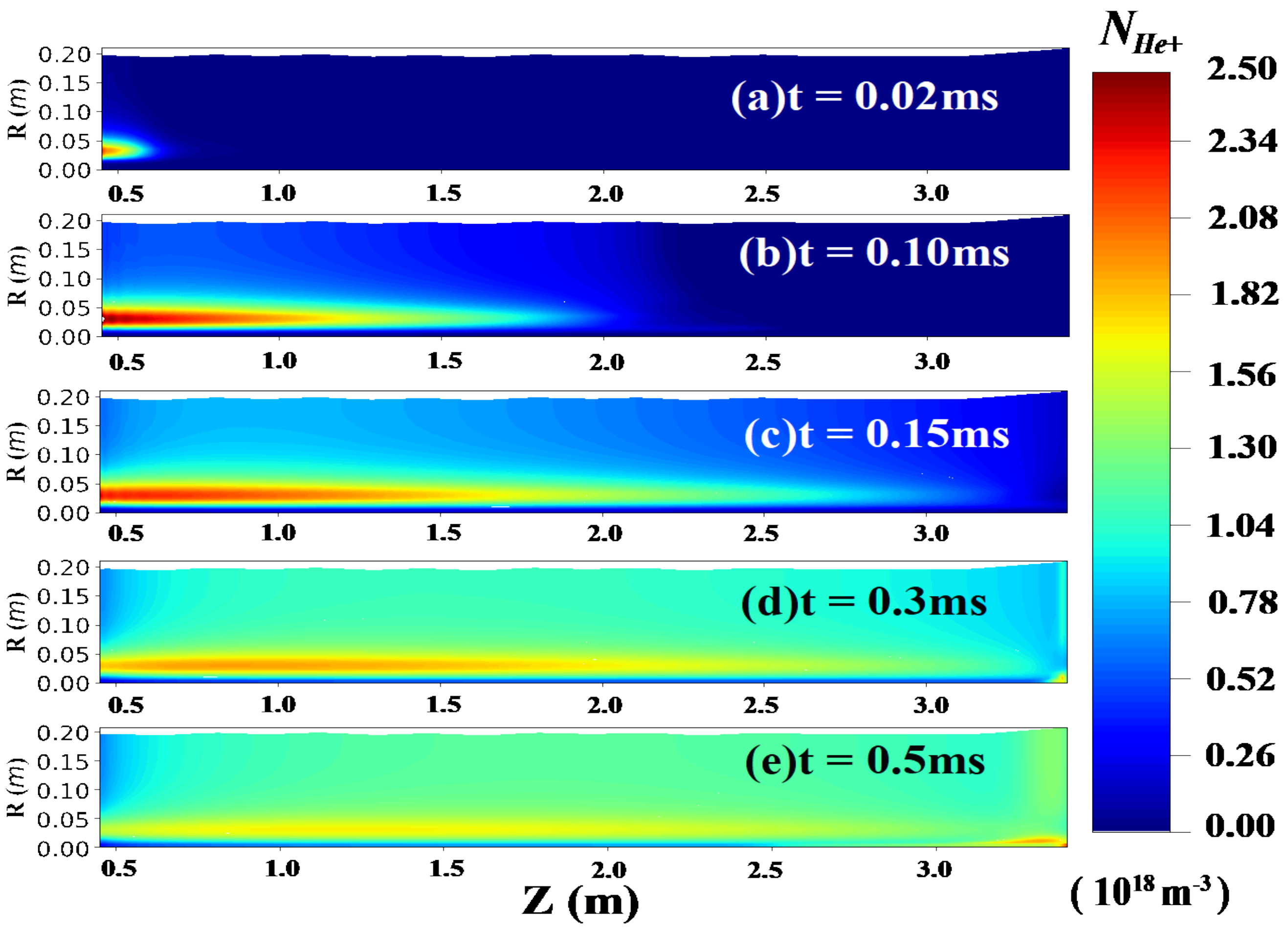

$D_\perp = 0.5\ m^2 s^{-1}$, $\chi_{\perp i,e} = 1.0\ m^2 s^{-1}$, R = 0.75,
Γ_{source}^{D+} =1.5 ×10^{21} D^+ s^{-1}, $\Gamma_{source}^{He} = 4.0 \times 10^{20}$He s^{-1}.

- At $t = 0.02$ ms the helium atom is ionized and reaches $1.628 \times 10^{18} m^{-3}$ near the gas inlet.
- At $t = 0.135$ ms, He+ reaches the target for the first time
- It reaches a maximum of about $2.5 \times 10^{18} m^{-3}$ at about t = 0.09 ms, and then N_{He+} begins to decrease over time
- At t = 0.27 ms, the N_{He+} near the gas charging port decreases obviously, but there is obvious He^+ accumulation in the whole device due to the recycle target

Helium injection can control target thermal load

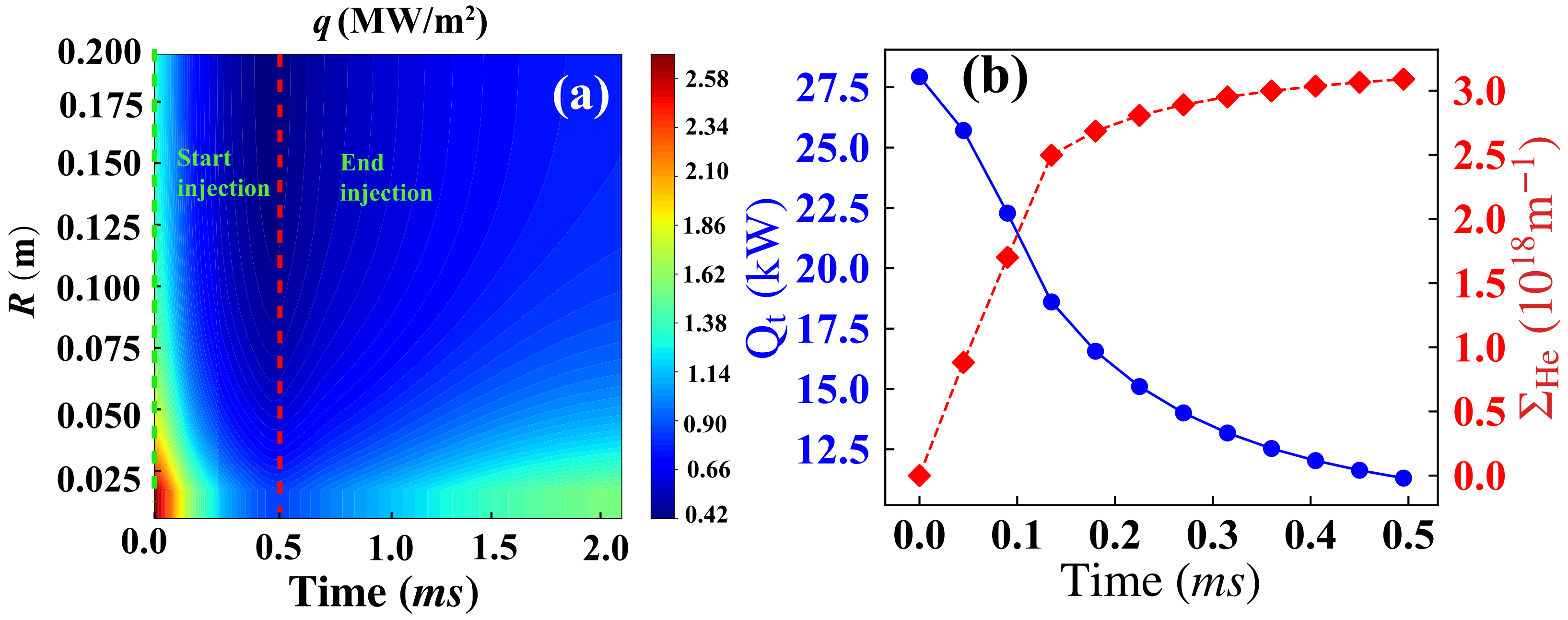

$Q_{ion} = VE_{ion}S_{ion} = VE_{ion}N_e\upsilon_{He}$

E_{ion} is ionization energy loss,

$\upsilon_{He} = N_{He} < \sigma_{He}V_{th,e} >$,

V is the simulation area,

N_{he} is impurity density, $\Sigma_{He} = VN_{He}$

- Q_t is inversely proportional to the number of He atoms in the simulation region Σ_{He}. With the increase of injection time, the Q_t and q of the whole target plate continue to decrease, and begin to stabilize after reaching a dynamic balance.

Outline

Conclusions and Future Plans

Conclusions

- Based on BOUT + +, a new LPD module is developed to simulate linear devices.
- For the first time, the LPD module is used to simulate the plasma transport in MPS-LD, and the main plasma parameters are obtained. And the corresponding verification was carried out.
- The smaller $D_{\perp}$ is beneficial to reduce the particle beam width, so the particle flux and the corresponding energy flux are significantly enhanced, while $\chi_{\perp i,e}$ only affects the energy flux.

Future plan:

- ✓ The neutral transport model need to be optimized to simulate plasma-neutral collisions more accurately.
- ✓ The impact of drifts on edge plasma transport in the LPD will be studied, especially on the plasma beam size.

Thank you for your attention